Generation and distribution of endothelium-derived contractile forces and their impact on vascular permeability

Valent, E.T.

2016

document version
Publisher's PDF, also known as Version of record

Chapter 4

ROCK2 primes the endothelium for vascular hyperpermeability responses by raising baseline junctional tension

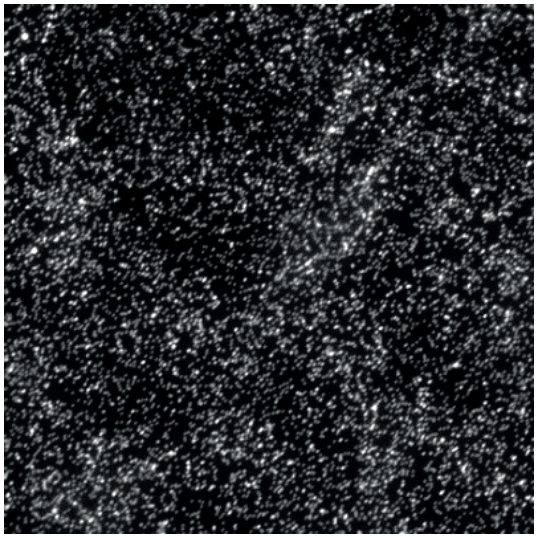

Erik T. Valent*, Cora M.L. Beckers*, Nebojsa Knezevic*, Mohammad Tauseef, Ramaswamy Krishnan, Kavitha Rajendran, C. Corey Hardin, Jurjan Aman, Jan van Bezu, Paul Sweetnam, Victor W.M. van Hinsbergh, Dolly Mehta, Geerten P. van Nieuw Amerongen

Vascular Pharmacology 2015; 70: 45–54

* Authors contributed equally to this manuscript

Abstract

Rho kinase mediates the effects of inflammatory permeability factors by increasing actomyosin-generated traction forces on endothelial adherens junctions, resulting in disassembly of intercellular junctions and increased vascular leakage. In vitro, this is accompanied by the Rho kinase-driven formation of prominent radial F-actin fibers, but the in vivo relevance of those F-actin fibers has been debated, suggesting other Rho kinase-mediated events to occur in vascular leak. Here, we delineated the contributions of the highly homologous isoforms of Rho kinase (ROCK1 and ROCK2) to vascular hyperpermeability responses. We show that ROCK2, rather than ROCK1 is the critical Rho kinase for regulation of thrombin receptor-mediated vascular permeability. Novel traction force mapping in endothelial monolayers, however, shows that ROCK2 is not required for the thrombin-induced force enhancements. Rather, ROCK2 is pivotal to baseline junctional tension as a novel mechanism by which Rho kinase primes the endothelium for hyperpermeability responses, independent from subsequent ROCK1-mediated contractile stress-fiber formation during the late phase of the permeability response.

Introduction

Numerous pathological conditions including life-threatening sepsis and acute respiratory distress syndrome (ARDS) are characterized by endothelial barrier failure.[1] The sequelae include uncontrolled fluid extravasation and edema.[1,2] Under acute inflammatory conditions, the post-capillary venules in particular become leaky, whereas in ARDS the alveolar-capillary barrier is the major site of leakage. Despite increasing incidence of sepsis [3] and high mortality rates in ARDS, no treatment is currently available to combat endothelial barrier disruption in these diseases.[1]

Endothelial barrier function is controlled principally by cytoskeletal elements that -in addition to local signaling events that weaken the junctions- orchestrate intercellular junctional complexes, and facilitate cell-matrix adhesion.[2] Dysfunction of the endothelial barrier can be elicited through activation of specific receptors by vasoactive agents such as thrombin and vascular endothelial growth factor (VEGF), as well as by interaction of the endothelium with leukocytes. Thrombin-induced signaling via its receptor PAR1 –which is short for protease-activated receptor 1- involves several signaling mechanisms that are simultaneously activated, including the influx of calcium ions, the activation of small Rho GTPases, activation of various kinases, and phosphorylation of (junctional) proteins. Among the small GTPases, RhoA is mainly involved in inducing endothelial hyperpermeability, whereas Rac1, Cdc42 and Rap1 contribute to enforcement of an intact barrier function.[4]

A key effector molecule of RhoA in regulating vascular permeability is Rho kinase. It has been well-appreciated that enhanced Rho kinase activity upon stimulation by inflammatory mediators such as thrombin has a strong barrier-disruptive effect.[5,6] However, basal Rho kinase activity is also involved in maintenance of barrier integrity.[7,8] Initial studies in endothelial cells (ECs) showed that transduction of a dominant-negative Rho kinase markedly reduced thrombin-induced formation of F-actin fibers through inhibition of the myosin phosphatase, serving as a paradigm for Rho kinase-mediated vascular hyperpermeability.[9] Yet, their *in vivo* relevance remained uncertain and has been debated for the microcirculation.[10,11] In cell models, Huveneers et al. showed that the agonist-induced radial F-actin fibers transmit tension to the endothelial junctions.[12] Indeed, pharmacological inhibition of Rho kinase reduces tension to the junctions, and ablates thrombin-induced hyperpermeability of endothelial monolayers by about 50%.[6] The remaining Rho kinase-independent part of the *in vitro* endothelial hyperpermeability involves regulation by protein tyrosine kinases and protein kinase C zeta.[13,14] In animal models, inhibitors of Rho kinase reduced vascular hyperpermeability induced by vaso-active agents such as VEGF, endotoxin (LPS) and thrombin even more effectively than *in vitro*.[15,16] But to the contrary, recent reports indicated that treatment of rats with the Rho kinase inhibitor fasudil, while effective in reducing LPS-induced permeability, improving survival in sepsis and preventing ARDS,[17] by itself promoted vascular leakage of macromolecules.[18] Taken together, these data suggest the presence of distinct and sometimes even opposing Rho kinase activities determining endothelial morphology and function.

In an attempt to resolve this discrepancy we turned to two distinct isoforms of Rho kinase, ROCK1 and ROCK2, encoded by two different genes.[19] These isoforms are highly homologous except for their PH domains. Their human forms share 64% sequence identity with 89% identity in the catalytic domain.[19] Given their high sequence similarity it is not surprising that available inhibitors do not distinguish between the two ROCK isoforms, except for the ROCK2 inhibitor SLx-2119, also known

as KD025, showing 200-fold higher selectivity toward ROCK2 (IC_{50} 105 nmol/L) compared to ROCK1 (IC_{50} 24 micromol/L).[20]

Analysis of Rho kinase knockout-mice suggest that there is no compensation for the loss of either isoform by the other: ROCK2-/- mice show a high fetal death rate [21] while ROCK1-/- die early after birth,[22] but ROCK1 null animals that survive develop normally. The developmental effects associated with ROCK1 and ROCK2 deficiency have limited the use of these animals to evaluate the functions of these molecules in physiology and disease in an isoform-specific manner. Also, most pharmacological inhibitors lack isoform specificity.

Rho kinase is involved in many basic vascular activities such as cellular migration, angiogenesis, and development of tone. Evidence has accumulated over the past decade that enhanced activity of Rho kinase plays an important role in many vascular pathologies including (pulmonary) hypertension, atherosclerosis, diabetes, and vascular leak.[23,24] ROCK isoform-specific regulation has been indicated for some of them.[25,26]

Given their discrete form and function, we hypothesized that specifically targeting a single Rho kinase isoform in anti-vascular leak therapy would be an effective and novel strategy. Accordingly, using a combination of in-vitro and in-vivo experiments, we investigated the individual contributions of ROCK1 and ROCK2 to the regulation of endothelial barrier permeability.

Materials & Methods

Sources of reagents are listed in the expanded Materials and Methods section in the online data supplement section.

Animal studies

All animal studies were approved by the Institutional Animal Care Committee of the University of Illinois. To deliver siRNA in the mouse lung, cationic liposomes were made using a mixture of dimethyldioctadecyl-ammonium bromide (DDAB) and cholesterol in chloroform, as described previously.[52] Control, ROCK1 or ROCK2 siRNA (75 µg) or ROCK1 + ROCK2 (37.5 µg each siRNA) were mixed with 100 µL of liposomes. The mixture of liposomes and siRNA were injected intravenously (via retro-orbital injection) into C57/Bl6 mice. After 48 hrs mice were used for determining lung microvascular permeability or were used for immunoblotting and immunohistochemistry analysis.

To assess lung capillary leakage, PAR1 specific peptide (TFRLLN) (1 mg/kg) was injected retroorbitally followed by injection of Evans blue conjugated albumin (EBA) (20 mg/kg) as described.[53] After 30 min, mice were sacrificed and blood was collected from the right ventricle into heparinized syringes. Right lung lobe was homogenized as described.[53] Lung homogenates and plasma were incubated with 2 volumes of formamide (18 hr, 60°C), centrifuged at 5,000 x *g* for 30 min, and the optical density of the supernatant was determined spectrophotometrically at 620 nm and at 740 nm (to correct for hemoglobin). EBA extravasation was calculated as the ratio of EBA extravasated in lung versus that in plasma. To determine lung weights, left lungs from the same mice used for EBA extravasation were excised and completely dried in the oven at 60°C overnight for calculation of lung wet-dry ratio.

In vitro studies

Human pulmonary microvascular endothelial cells (HPMVECs) isolated from human lung tissue and human umbilical vein endothelial cells (HUVECs) were isolated, cultured, and characterized as previously described.[8] ECs were transfected with short interfering (si) RNA duplexes using Amaxa technology.

Barrier function was evaluated by the transfer of HRP across EC monolayers grown on polycarbonate filters of the Transwell system.[8] Alternatively, Electrical cell substrate impedance sensing (ECIS) was used to measure transendothelial electrical resistance (TEER) in confluent monolayers. For 3D-Digital fluorescence imaging microscopy, HUVECs were examined with a ZEISS Axiovert 200 Marianas inverted microscope.

Endothelial monolayer contraction was measured by monolayer traction microscopy.[31] Intercellular stresses were mapped by monolayer stress microscopy.[35]

Statistical analysis

All data are reported as mean ± SD. Comparisons between 2 experimental groups were made by student t-test and between >2 groups by one way ANOVA with bonferoni post-hoc test. Differences in mean values were considered significant at $p < 0.05$.

Results

Efficacy of ROCK1 and ROCK2 depletion by siRNA treatment in vitro and in vivo

In vitro experiments were performed throughout this study with human umbilical vein endothelial cells (HUVECs). Key findings were verified in primary human pulmonary microvascular endothelial cells (HPMVECs) and presented in the online supplement.

The efficacy of siRNAs to downregulate ROCK protein expression in HUVECs was monitored by Western blotting of cell lysates obtained at 48 hrs after transfection. A net decrease in ROCK protein expression in each experiment of at least 90% was observed in ROCK1-silenced ECs and of 75% in ROCK2-silenced ECs (see Figure 1A for representative Western blot).

To test whether the siRNAs directed at human ROCK sequences were also effective in downregulating mouse ROCK1 and ROCK2, mouse NIH3T3 cells were used as a model cell system. The siRNAs directed to human ROCK1 and ROCK2 were less effective in downregulating mouse ROCK protein expression (data not shown). Therefore, new siRNAs were designed directed to mouse ROCK sequences (see materials & methods), resulting in a >80% downregulation of mouse ROCK1 and ROCK2 protein expression *in vitro* (see figure 1B for a representative Western blot).

Immuno-histochemical staining of both ROCK1 and ROCK2 revealed their abundant expression in endothelial cells of large pulmonary arterioles as well as in the small capillaries of the mouse lung (Figure 1C). Their expression was selectively downregulated 48 hrs after retro-orbital injection of the corresponding siRNAs as evidenced by semi-quantitative immuno-histochemical analysis of arteriolar ROCK1 expression (Figure 1D,E).

Silencing of ROCK1 and ROCK2 reveals differential involvement in endothelial permeability

To evaluate the contributions of ROCK1 and ROCK2 to permeability changes of human endothelial monolayers, HUVECs were grown *in vitro* on porous filters, and permeability for the tracer HRP was

measured. The thrombin-induced endothelial hyperpermeability of these monolayers is for about 40-60% dependent on Rho kinase, representing the *in vivo* PAR1-mediated vascular permeability, whereas the remainder is independent of Rho kinase, involving other signaling pathways as outlined in the introduction.[2,6]

Thrombin elicited a 7.2 ± 0.7-fold increase in the passage of the tracer molecule HRP (Figure 2A). It is known that PAR1-activating peptides recapitulate the pro-inflammatory effects of thrombin in endothelial cells,[27] which we confirmed *in vitro* where PAR1-peptide and thrombin evoked a comparable transient decrease in endothelial barrier function (Supplementary figure S1). Silencing of ROCK1 did not affect thrombin-induced permeability, whereas silencing of ROCK2 significantly reduced thrombin-induced permeability (Figure 2A). Simultaneous silencing of ROCK1 and ROCK2 further reduced the absolute or net thrombin-induced increase in permeability, and showed an almost similar effect as pharmacological inhibition by Y-27632.

To evaluate the contribution of ROCK1 and ROCK2 to PAR1-mediated vascular hyperpermeability *in vivo*, ROCK1 or ROCK2 siRNA-transduced mice were stimulated with PAR1-peptide for 30 minutes. The pulmonary microvascular permeability following PAR1-stimulation was determined by measuring Evans Blue-conjugated Albumin (EBA) extravasation (Figure 2B).

None of the siRNA treatments affected baseline permeability. PAR1-peptide evoked a 2-fold increase in EBA extravasation. Silencing of ROCK1 had no effect on PAR1-mediated EBA leakage. Silencing of ROCK2 decreased the PAR1 permeability response by about 50%, while silencing of both ROCK1 and ROCK2 almost completely prevented the increase in EBA extravasation upon treatment with a PAR1-peptide. The potent pharmacological pan-Rho kinase inhibitor Y-27632 was equally effective as silencing of both ROCK1 and ROCK2. These findings were supported by comparable changes in lung wet-dry weight ratios (data not shown).

Together, these data indicate that ROCK2 primarily regulates the thrombin receptor-mediated vascular hyperpermeability response both *in vitro and in vivo*. ROCK1 is dispensable for this hyperpermeability response, but silencing of ROCK1 enforced the attenuating effect of silencing of ROCK2. These data point to distinct roles of ROCK1 and ROCK2 in the regulation of vascular hyperpermeability.

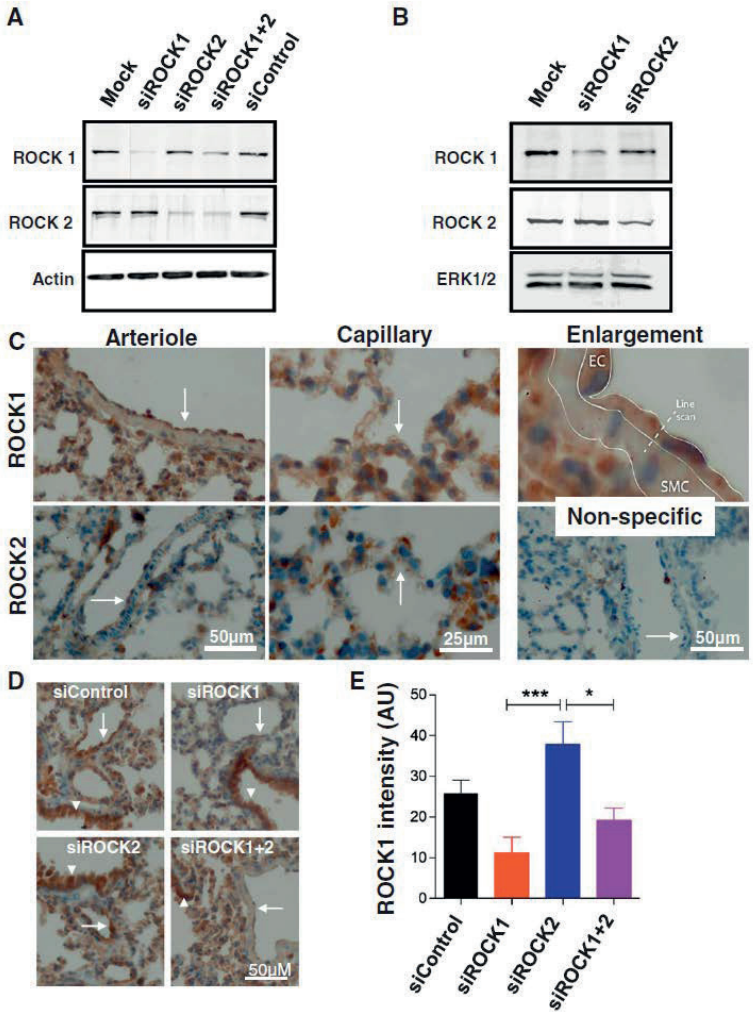

Fig. 1. Efficacy of ROCK1 and ROCK2 depletion by siRNA treatment in vitro and in vivo. A: Effect of ROCK1 and/or ROCK2 siRNAs on ROCK protein expression in cultured HUVECs. Representative Western blot showing changes in the expression of ROCK1 and ROCK2 48 h after transfection of HUVECs with ROCK1 or ROCK2 siRNA(s). Blot was probed with ROCK1 (upper panel) or ROCK2 (middle panel) antibodies to verify reduced ROCK expression upon siRNA transfection. Blot was reprobed for actin as a loading control (lower panel). Similar results were obtained in 8 independent experiments. B: Effect of ROCK1 and/or ROCK2 siRNAs on ROCK protein expression in cultured mouse NIH3T3 cells. Representative Western blot showing changes in the expression of ROCK1 and ROCK2 48 h after transfection with ROCK1 or ROCK2 siRNA(s). Blot was probed with ROCK1 (upper panel) or ROCK2 (middle panel) antibodies to verify reduced ROCK expression upon siRNA transfection. Blot was reprobed for ERK1/2 as a loading control (lower panel). Similar results were obtained in 3 independent experiments. C: Representative immune-histochemical staining of ROCK1 and ROCK2 demonstrating their expression in the mouse pulmonary vasculature. ROCK1 and ROCK2 are present in various cell types including endothelial cells. Arrows point to the endothelium at the luminal site of the arteriolar vessel wall (left panels) and to capillaries (middle panels). The upper right panel highlights the endothelial expression of ROCK1. For quantification, line scans were drawn over the vessel wall from the lumen to the cytoplasm of underlying smooth muscle cells. The lower right panel shows non-specific control staining. Left panels: bar = 50 µm; middle panels: bar = 25 µm. D: Effect of ROCK1 and/or ROCK2 siRNAs on ROCK1 protein expression of pulmonary vascular endothelium. The lungs were harvested 48 h

after injection of liposomes conjugated with indicated siRNA, as described in the Materials & methods section. Immuno-histochemical staining for ROCK1 was reduced in the endothelium of arterioles (arrows) of ROCK1, but not ROCK2 transduced mice, whereas bronchiolar ROCK1 expression was not affected (arrow heads). Bar = 50 µm. E: Intensity of ROCK1 staining, quantified according to the description in the Materials & methods section. Values represent differences in intensity of staining between endothelial cells and vascular smooth muscle cells. Mean ± SEM of 4–6 vessels from 2 mice per treatment group. *p < 0.05, ***p < 0.001.

Specific pharmacological inhibition of ROCK2 attenuates endothelial hyper-permeability

The role of ROCK2 in regulating the endothelial barrier function was further explored by using the ROCK2-selective inhibitor SLx-2119.[20,28] The effects of SLx-2119 were compared to the effects of the pan-Rho kinase inhibitor Y-27632. Probing ROCK2 Ser1366 phosphorylation as a surrogate marker for ROCK2 activation status [29] showed a rapid and transient activation of ROCK2 upon stimulation with thrombin (Figure 2C inset). ROCK2 activation was entirely prevented by SLx-2119 as well as by downregulation of ROCK2 supporting the specificity of the inhibitor as well as the siRNA sequences, whereas silencing of ROCK1 had no effect of ROCK2 activation (Supplementary figure S2).

Pretreatment with SLx-2119 reduced thrombin-induced HRP passage to 74±12% of thrombin-induced HRP flux in the absence of inhibitors (t= 30 min after thrombin stimulation, 12 filters from 4 different donors; $p<0.05$), to a similar extent as silencing of ROCK2 (77±15%). Y-27632 tended to slightly further inhibit thrombin-induced HRP passage (to 62±6%). Detailed analysis (Figure 2C left panel) of the time-dependency of the ROCK2 effects indicated that ROCK2 mainly was involved in the early phase of the thrombin-induced endothelial permeability changes, whereas only in the later phase ROCK1 additionally contributed to barrier dysfunction (Figure 2C right panel).

Finally, these findings were verified in human pulmonary microvascular endothelial cells (Supplementary figure S3). In these primary cells, the role of Rho kinase in thrombin-induced permeability was even more prominent during the early phase of the permeability response to thrombin: SLx-2119 dose-dependently attenuated thrombin-induced HRP passage, to an almost similar extent as the pan-Rho kinase inhibitor Y-27632.

Thus, specific pharmacological inhibition of ROCK2 attenuates the disruption of human endothelial barrier integrity, in particular during the early phase of disruption. The differences in the time profiles for the involvement of ROCK1 and ROCK2 in endothelial hyper-permeability confirm distinct mechanistic contributions to the regulation of endothelial barrier function.

ROCK1, but not ROCK2 mediates the formation of thrombin-induced F-actin cytoskeletal stress fibers

The Rho kinase-dependent formation of contractile F-actin stress fibers is a remarkable feature of thrombin-stimulated ECs *in vitro*, but their presence in intact microvessels is debated.[30] Therefore, it remains to be determined if and how F-actin stress fibers play a role in endothelial permeability.

To evaluate whether ROCK2 mediates the thrombin-induced permeability changes through the formation of contractile F-actin stress fibers, endothelial monolayers were stained for F-actin with rhodamine-phalloidin and co-stained for VE-cadherin. HUVECs in a continuous monolayer of closely attached cells were characterized by a cortical F-actin band (Figure 3) and the presence of some cytoplasmic F-actin filaments. Stimulation with thrombin for 30 minutes induced a loss of the peripheral F-actin rim, but an overall increase in F-actin staining, especially of F-actin stress

fibers (Figure 3 arrows). Both changes in the F-actin cytoskeleton were attenuated by 30 minutes pretreatment with Y-27632. Surprisingly, pretreatment with SLx-2119 had no obvious effect on the thrombin-induced F-actin reorganization, indicating that ROCK2 is dispensable for the formation of contractile F-actin stress fibers. Similarly, depletion of ROCK2 by siRNA treatment did not prevent stress fiber formation, whereas depletion of ROCK1 almost completely prevented their appearance (Supplementary figure S4).

The distribution of VE-cadherin was not altered by ROCK2 inhibition, neither was the connection of thrombin-induced radial F-actin fibers to VE-cadherin affected in the focal adherens junctions (Figure 3).[12] Importantly, inter-endothelial gaps did form in ROCK2-inhibited HUVECs, indicating that the radial F-actin fibers were functionally intact, but HUVECs showed a more pronounced protrusive activity filling the gaps at their basal site (compare boxes in Figure 3; these boxes are enlarged in supplementary figure S5A,B).

Thus, ROCK2, but not ROCK1, is dispensable for the formation of thrombin-induced F-actin stress fibers.

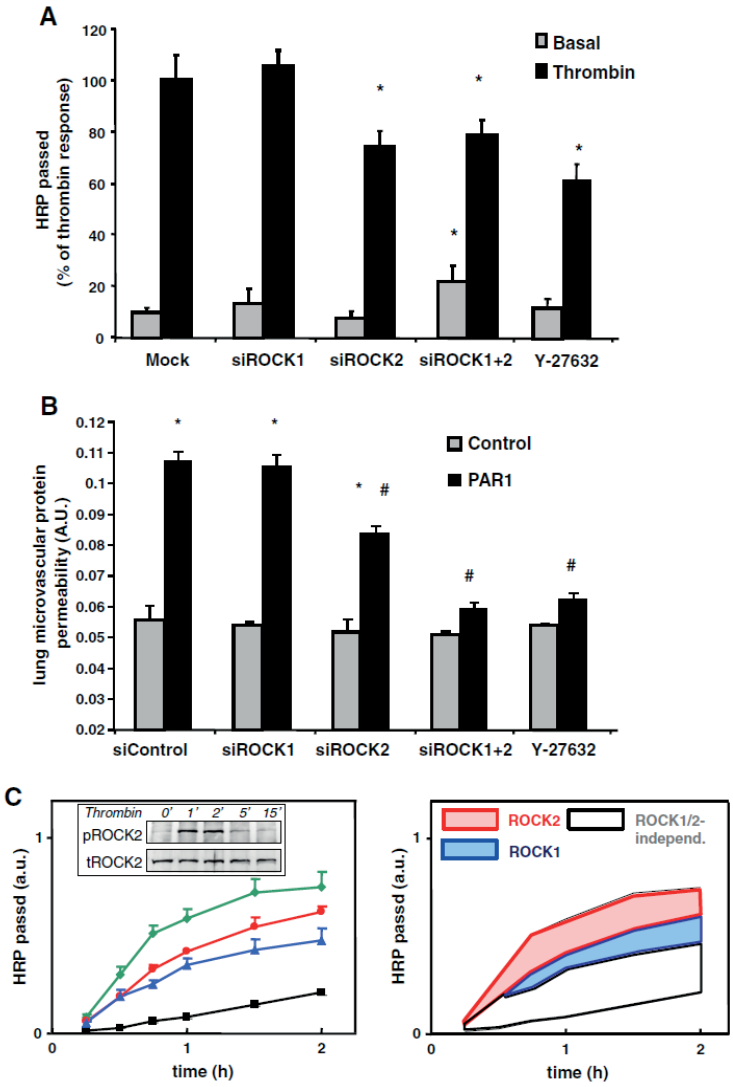

Fig. 2. ROCK1 and ROCK2 differentially regulate PAR1-mediated endothelial permeability in vitro and in vivo. A: Effects of ROCK silencing on the passage of HRP across HUVEC monolayers under basal conditions and 30 min after exposure to 1 U/mL thrombin. 48 h after transfection with the indicated siRNAs, cells were preincubated for 1 h in medium-199 + 1% HSA and cumulative HRP passage over the 30min period in the presence or absence of thrombin was measured subsequently as described in the Materials & methods section. For comparison, the effect of the pan-Rho kinase inhibitor Y-27632 is shown (30 min pre-incubation). Values are the mean+ SD (4 independent experiments performed in triplicate. Each experiment was performed with HUVECs isolated from a different donor). * indicates significance from appropriate control group (p b 0.05). B: ROCK2 is critically involved in PAR1-mediatedmouse lung microvascular permeability. PAR1-peptide (TFLLRN) 1 mg/kg or control peptide (FTLLRN) was injected together with Evans blue albumin retroorbitally into C57/Bl6 mice, 48 h after injection of liposomes conjugated with indicated siRNA. After 30min, Evans blue-albumin extravasation from the lungs was determined as described in the Materials & methods to quantify lung microvascular protein permeability. Y-27632 (10mg/kg body weight) was administered intravenously. Data represent mean ± SD of n=4 mice per group. * indicates significance

between PAR1 treatment and appropriate control peptide group within the same group ($p < 0.05$); # indicates significance from mice injected with control siRNA after PAR1 challenge ($p < 0.05$). C: Time-dependent effects of Rho kinase inhibitors on the passage of HRP across control and thrombin-stimulated human umbilical vein. Left panel: Confluent monolayers were preincubated for 1 h in medium 199 + 1% HSA, pre-treated with 10 μM Y-27632 (blue), 10 μM SLx-2119 (red) or sham-treated (green) for 30 min. Subsequently, the cumulative HRP passage across the monolayers was measured in the presence of 1 U/mL thrombin, as described in the Materials & methods section. The baseline permeability of monolayers that were not treated with thrombin is shown for comparison (black). The right panel is color-shaded to better visualize the individual contributions of ROCK1 and ROCK2 to the thrombin-enhanced permeability. Values are the mean+SD (experiment performed in triplicate). Inset: ROCK2 is transiently activated in HUVECs upon thrombin-stimulation. Representative Western blot showing changes in the phosphorylation of ROCK2 upon stimulation with 1 U/mL thrombin for the indicated time points. Blot was probed with a phospho-specific ROCK2 antibody (upper panel) and reprobed with a total ROCK2 antibody (lower panel) as a loading control. Similar results were obtained in 3 independent experiments.

ROCK2 is a pivotal determinant of baseline intercellular forces

Since F-actin staining does not provide information on whether or not the formed F-actin stress fibers are functional, we sought to directly measure the thrombin-induced contractile forces. We applied a recently reported technique called monolayer traction microscopy to endothelial monolayers.31 Traction forces exerted by endothelial cells on their extracellular matrix are counter-balanced at the level of the cell-cell junctions. The magnitude of these tractions are proportionally related to the cell-cell forces as a constant fraction (~0.5).32,33 The magnitude of these tractions is also proportionally related to the basal cellular tone or pre-stress.34 HUVECs grown to confluent monolayers were characterized by baseline traction forces of a high magnitude and spatial heterogeneity (Figure 4 A, B). The baseline traction forces were dramatically ablated by Y-27632, and to a lesser extent by SLx-2119 (Figure 4B). To directly demonstrate that the measured traction forces reflect intercellular forces, intercellular stress maps were generated by a novel technique called monolayer stress microscopy.35 Both ROCK inhibitors largely reduced baseline intercellular stresses (Figure 4C).

In sham-treated control cells, the baseline traction forces were significantly enhanced in response to thrombin. These thrombin-induced force enhancements were significantly ablated by pre-treatment with Y-27632 (Figure 4D, E). In contrast, pretreatment with the ROCK2-selective SLx-2119 did not affect the net thrombin-induced forces (Figure 4D, E). Similarly, simultaneous silencing of ROCK1 and ROCK2 largely inhibited the thrombin-enhanced contractile force enhancements, whereas silencing of ROCK2 alone did not affect thrombin-induced forces (Supplementary Figure S6).

Thus, ROCK2 activity is an important determinant of baseline monolayer intercellular forces, but is not involved in thrombin-induced contractile force enhancements.

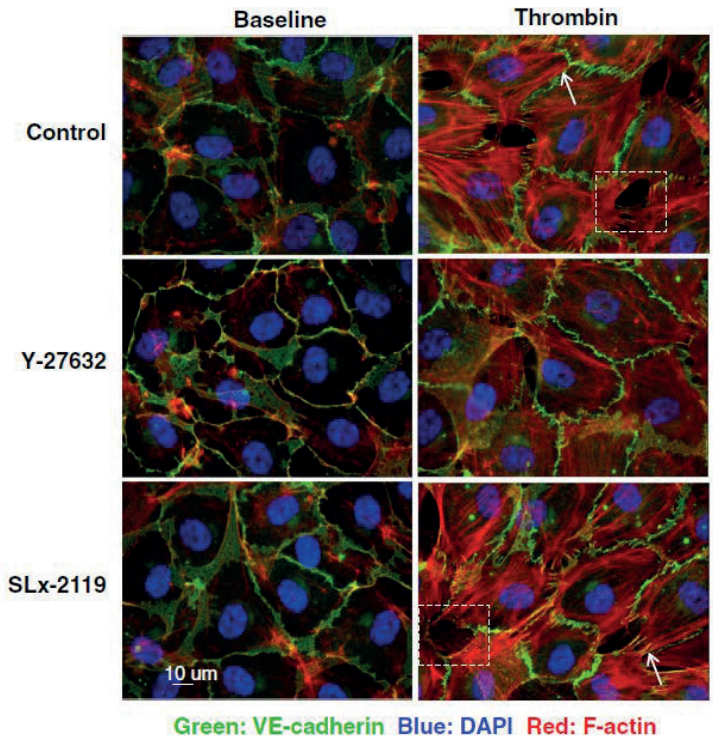

Fig. 3. ROCK2 is not essential for thrombin-induced formation of radial F-actin fibers. Y-27632, but not SLx-2119 prevented thrombin-induced cytoskeletal reorganization. F-actin (red) and VE-cadherin (green) staining of HUVECs grown on glass cover slips; cells were counter-stained with DAPI (nuclear staining). HUVECs were preincubated for 1 h in medium 199 + 1% HSA in the absence or the presence of 10 µmol/L of the Rho kinase inhibitors SLx-2119, and Y-27632 where indicated and stimulated for 30 min with 1 U/mL thrombin or sham-treated. Arrows point to radial F-actin fibers. Enlargements of boxed areas are shown is Supplementary Fig. S5A. Similar results were obtained in 4 independent experiments. Bar = 10 µm.

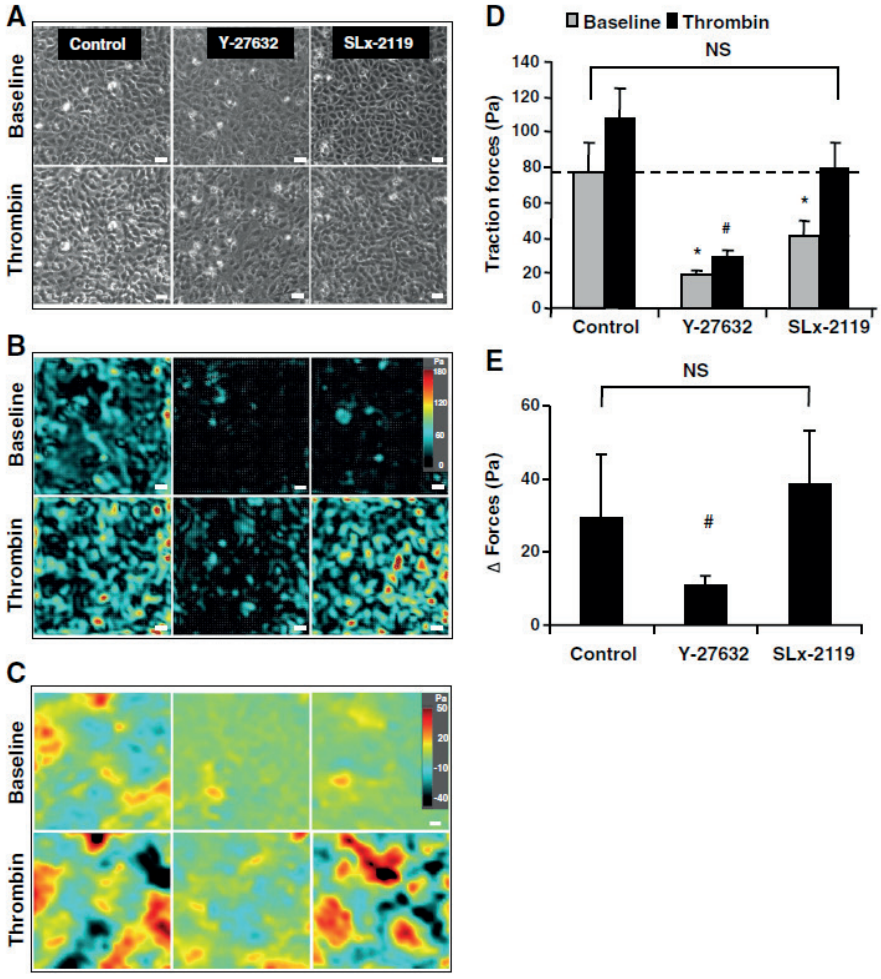

Fig. 4. Inhibition of ROCK2 reduces basal traction forces but does not affect thrombin-induced contractile stress enhancements. A, B, C: Representative phase contrast images (A), cell–substrate traction stress maps (B) and intercellular stress maps (C) at baseline and 10min post-thrombin treatment from each group. HUVEC monolayers were pretreated with the indicated Rho kinase inhibitors for 30min and subsequently stimulated with thrombin (1 U/mL) for 10min or sham-treated. Traction stress maps presented in (B) belong to the monolayers presented in (A). Bar = 50 µm. D: Quantification of the effects of different Rho kinase inhibitors on traction forces across all groups, presented as RMS traction stresses. Values are the mean ± SD of 4 independent determinations in duplicate. *p < 0.05 basal RMS traction stresses of monolayers pretreated with Rho kinase inhibitors vs control monolayers. #p < 0.05 thrombin-induced RMS traction stresses of monolayers pretreated with Rho kinase inhibitors vs control monolayers. E: Bar graph showing the effect of the different Rho kinase inhibitors on the net thrombin-induced change in RMS traction stresses calculated from the data presented in (B) (i.e. RMS traction stresses at t = 10 min after thrombin treatment minus RMS traction stresses at baseline). # indicates p < 0.05 thrombin-treated monolayers pretreated with vs without Rho kinase inhibitors.

ROCK2 mediates baseline, but not thrombin-mediated changes in trans-endothelial electrical resistance (TEER)

We next aimed to investigate whether inhibition of ROCK2 is barrier-protective through enforcement of the baseline characteristics of the endothelial barrier.

Silencing of ROCK2 slightly reduced the baseline flux of HRP across endothelial monolayers (0.7 ± 0.2-fold, see also Figure 2A), whereas silencing of ROCK1 tended to increase basal permeability (1.3 ± 0.6-fold). These trends did not reach statistical significance, but suggested that ROCK1 and ROCK2 might have distinct roles in regulating basal endothelial permeability. Simultaneous silencing of ROCK1 and ROCK2 significantly doubled the HRP flux (2.0 ± 0.6 fold), in line with the previous finding 8,36 that prolonged inhibition of Rho kinase (10 microM Y-27632 for 48 hr) induced a similar disruption of baseline barrier integrity.

Next, we evaluated the effect of Rho kinase inhibitors on endothelial barrier integrity by measurement of trans-endothelial electrical resistance or TEER (Figure 5A and 5B). We utilized an electrical cell substrate impedance-sensing (ECIS) assay, as ECIS allows online monitoring of barrier function, with higher precision than tracer permeability measurements in the transwell assays do. However, it is important to realize that ECIS measurements do not replace tracer permeability measurements as ECIS measurements provide an indirect reflection of barrier function: changes in TEER are not necessarily accompanied by alterations in barrier properties towards larger molecules, i.e. they do not necessarily reflect actual changes in passage of tracers across the endothelium.

Analysis of the effect of the Rho kinase inhibitors on basal barrier integrity showed that inhibition of ROCK2 with SLx-2119 significantly elevated baseline electrical resistance (Figure 5A, B), whereas electrical resistance upon treatment with the pan-Rho kinase inhibitor Y-27632 was not elevated. Thus, inhibition of ROCK2 improves endothelial basal barrier integrity, whereas simultaneous inhibition of ROCK1 abolished this effect.

Next, we analyzed the effects of the Rho kinase inhibitors on the thrombin-induced changes in TEER. Thrombin induced a transient decrease in TEER, with a minimal TEER between 45 and 60 minutes showing a reduction of 64.1 ± 11.8%, which was followed by recovery of the monolayer (Figure 5A). Pretreatment with the pan-Rho kinase inhibitor Y-27632 largely attenuated the thrombin-induced decrease in TEER (Figure 5A). In contrast, pretreatment with SLx-2119 resulted in an upward shift of the entire curve, indicating that SLx-2119 increased the initial baseline TEER, without affecting the net thrombin-induced changes. This was further evidenced by analysis of the maximal thrombin-induced decrease in TEER (Figure 5C), which was almost entirely ablated by pre-treatment with Y-27632, but not affected by pretreatment with SLx-2119. Similarly, SLx-2119 improved basal barrier integrity in human pulmonary microvascular endothelial monolayers, but did not affect the thrombin-induced drop in TEER (data not shown).

Taken together, these data indicate that ROCK2 activity is critical for the development of a baseline isometric tone and enforcement of baseline barrier characteristics, but does not contribute to the thrombin-induced contractile force enhancements.

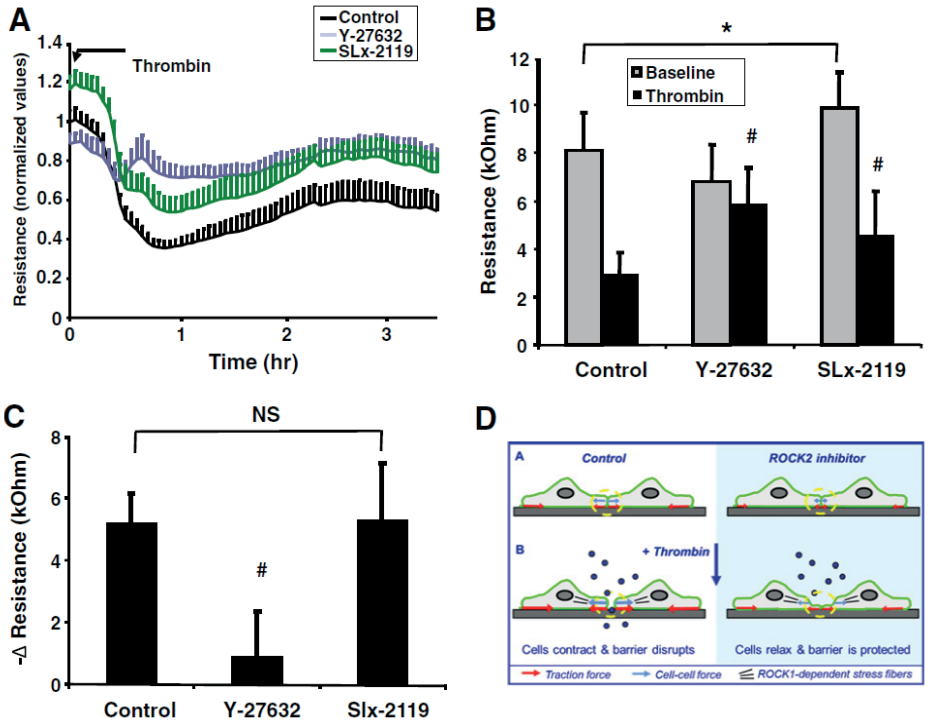

Fig. 5. Inhibition of ROCK2 affects baseline, but not thrombin-induced alterations in trans-endothelial electrical resistance. A: Graph representing the time course of the effect of Rho kinase inhibitors on trans-endothelial electrical resistance of HUVEC monolayers as measured by the ECIS method, see the Materials & methods section. Data are presented as normalized values for resistances of each individual well measured at t=0min. Values are the mean±SD of 16 cultures in 4 independent experiments. B: Bar graph showing that the effect of different Rho kinase inhibitors trans-endothelial electrical resistance at baseline and after stimulation with thrombin (t=30min). Data are presented as the absolute values of the same experiments shown in (A). *$p < 0.05$ basal resistance of monolayers pretreated with Rho kinase inhibitors vs control monolayers. #$p < 0.05$ resistance of thrombin-stimulated monolayers pretreated with Rho kinase inhibitors vs non-pretreated monolayers that were stimulated with thrombin. C: Bar graph showing the effect of the different Rho kinase inhibitors on the net thrombin-induced change in TEER calculated from the data presented in (B) (i.e. resistance at t=30 min after thrombin treatment minus resistance at baseline). # indicates $p < 0.05$ thrombin-treated monolayers pretreated with vs without Rho kinase inhibitors. D:Model depicting that inhibition of ROCK2 promotes vascular barrier stability through lowering of the force balance in endothelial junctions. See the Discussion section for a description of the details on how ROCK2 activity is pivotal to a critical junctional tension for opening of the endothelial barrier in response to inflammatory mediators. In addition, thrombin induces other changes such as a simultaneous decrease in Rac1 activity and changes in phosphorylation of intercellular adhesion proteins that are not shown for the sake of simplicity.

Discussion

The main finding of the present study is that the Rho kinase isoform ROCK2 mediates passive junctional tension in the endothelium as an entirely novel concept of regulating vascular hyperpermeability by Rho kinase, independent from the well-known role of Rho kinase in F-actin stress fiber formation. Inhibition of ROCK2 attenuates endothelial barrier dysfunction and pulmonary edema. Thus, selective pharmacological inhibition of basal traction forces might provide a novel approach to stabilize the endothelial barrier, and limit vascular leak during derailed inflammatory episodes. These findings shed new light on a longstanding controversy between physiologists and cell biologists whether or not Rho kinase-mediated F-actin stress fibers contribute to vascular hyperpermeability responses (Figure 5D).

In endothelial monolayers forces are exerted at cell-matrix interactions known as traction forces (indicated by the red arrows in Figure 5D) and at cell-cell interactions known as cell-cell or intercellular forces (indicated by the blue arrows). The intercellular forces account for nearly one-half of the overall forces in the monolayer and determine junctional tension born by the adherens junctions (upper left).[32,33] Evidence indicates that classical cadherins, including VE-cadherin are under tension.[37–40] Recently, Rac1 has been shown as a modulator of Rho kinase-mediated junctional tension.41 The present study shows that baseline forces are substantially reduced with ROCK2 inhibition (upper right), indicating that ROCK2 is a key molecule in the regulation of junctional tension at baseline. Upon stimulation with thrombin, overall forces increase, such that part of the junctions no longer can bear those forces. Cells start to contract and junctional complexes fall apart, resulting in opening of the barrier (lower left). The net increase in thrombin-enhanced contractile forces is not affected by ROCK2 inhibition. However, as these thrombin-induced contractile force enhancements in ROCK2-inhibited cells are now superimposed on a lower level of baseline junctional forces, the net result is a lower level of overall forces. These forces no longer reach a critical threshold necessary for disrupting junctional integrity and opening of the barrier for macromolecules (lower right). Such a critical threshold might be necessary for opening the vascular barrier under inflammatory conditions. At a later stage, F-actin stress fibers are formed in a ROCK1-dependent manner contributing to prolongation of the hyperpermeability reponse. Thus, ROCK2 activity is pivotal to a critical junctional tension for opening of the endothelial barrier when the interaction of junctional proteins is weakened in response to inflammatory mediators.

Both silencing as well as pharmacological inhibition of ROCK2 reduced thrombin-induced endothelial hyperpermeability. Similarly, in epithelial cells, ROCK2, but not ROCK1 mediated disassembly of the junctions.[42] However, another report indicated that ROCK1 mediated the early, but not late effects of TNFalpha on endothelial permeability, a finding hard to reconcile with the observation in the same report that ROCK2 was the primary Rho kinase activated in lungs of LPS-treated mice.[43,44] Unfortunately, the authors did not evaluate vascular permeability in these mice.

In the present study we observed that ROCK1 was dispensible for thrombin-induced endothelial hyperpermeability as long as ROCK2 is present in the ECs, but not vice versa. This points to a special form of compensation known as quantitative redundancy. In complete redundancy, absence or malfunction of either protein alone has no effect, but disruption of both proteins affects cellular behaviour.[45,46] In contrast, two proteins are quantitatively redundant when malfunction of the one

protein has no effect, as long as the compensating protein is functioning normally, but the effect of absence or malfunction of the other is exacerbated by absence of the former. Quenching of shared (inhibitory) factors by ROCK1 and ROCK2 provides an alternative explanation of the additive effects of silencing of ROCK1 in ROCK2-silenced ECs. In such a case the effects of ROCK1 are secondary and do not require direct involvement of ROCK1 in regulation of endothelial barrier integrity. Of interest, a minimal increase in ROCK1 activity has been reported during sepsis, but its functional role remains to be investigated.[43] The future development of ROCK1-specific inhibitors would provide a valuable tool to further delineate the role of ROCK1.

Another interesting aspect of the current study is the almost complete prevention of PAR1-induced vascular permeability in mice transduced with ROCK1 and ROCK2 siRNAs, that were characterized by a partial reduction in ROCK1/2 expression as was evidenced by immunohistochemistry. Similarly, in haplo-insufficient ROCK1 mice thrombin-induced ICAM1 expression was completely inhibited.[47] These findings indicate a critical threshold for Rho kinase expression and/or activity below which Rho kinase-dependent responses are severely hampered.

It should be emphasized that ROCK2 was not necessary for the thrombin-induced formation of F-actin stress fibers and force enhancements. Similarly, ROCK2, but not ROCK1 has been shown to be dispensable for stress fiber formation in vascular smooth muscle cells.[26] Stress fibers are considered as contractile F-actin filaments formed upon Rho kinase activation to prolong MLCK-initiated contraction.[48] As stress fibers are a characteristic feature accompanying many in vitro hyperpermeability responses, it is a wide-held assumption that they mediate the cellular contractile response leading to gap formation between ECs.[9] Our finding that a ROCK2 inhibitor reduces thrombin-induced permeability, while leaving the formation of F-actin stress fibers intact, challenges the paradigm that these stress fibers are necessary for prolonged Rho kinase-mediated endothelial permeability. Interestingly, recent data indicate that central F-actin fibers distinguishes the endothelial phenotype of adult arteries from veins.[49] Moreover, in intact microvessels in situ thrombin-induced F-actin fibers are smaller in size and in number,30 and in vivo a PAR1-peptide hardly induced the formation of stress fibers, whereas both stimuli resulted in enhanced vascular permeability.[30]

In epithelial cells, ROCK2 is complexed to adaptor protein cingulin in junctional complexes where it regulates tight junction formation.[50] It is tempting to speculate that ROCK2 in endothelium also enforces such interactions in the junctions. An attractive scenario for how ROCK2 could establish basal endothelial tension or prestress in the endothelium is recruitment to cortical F-actin through Shroom2 (Shrm2). Recent data indicate that Shrm2 is expressed within the endothelium, is localized to cortical actin and cell–cell adhesions, and contains a conserved Rho kinase binding domain.[51]

In conclusion, this is the first report addressing the individual contributions of ROCK1 and ROCK2 to in vivo vascular leak. It points to a major role of ROCK2 in vascular hyperpermeability responses through regulation of baseline tension in the adherens junctions independent from the involvement of F-actin stress fibers and reinforces the notion that Rho kinase is an attractive target in future anti-vascular leak therapy.

Sources of funding

GPvNA was supported by The Netherlands Heart Foundation (The Hague, grant 2003T032 and 2011T072), RK in part by the Parker B. Francis foundation, DM by HL71784 and CCH in part by the National Institutes of Health (NIH 1K25HL111212).

Disclosures: None

References

1. Goldenberg NM, Steinberg BE, Slutsky AS, Lee WL. Broken barriers: a new take on sepsis pathogenesis. *Science translational medicine*. 2011;3(88):88ps25.
2. Mehta D, Malik AB. Signaling mechanisms regulating endothelial permeability. *Physiological reviews*. 2006;86(4):279–367.
3. Martin GS, Mannino DM, Eaton S, Moss M. The epidemiology of sepsis in the United States from 1979 through 2000. *The New England journal of medicine*. 2003;348(16):1546–1554.
4. Spindler V, Schlegel N, Waschke J. Role of GTPases in control of microvascular permeability. *Cardiovascular research*. 2010;87(2):243–253.
5. Birukova AA, Smurova K, Birukov KG, Kaibuchi K, Garcia JGN, Verin AD. Role of Rho GTPases in thrombin-induced lung vascular endothelial cells barrier dysfunction. *Microvascular Research*. 2004;67:64–77.
6. Amerongen GPVN, Delft S Van, Vermeer MA, Collard JG, Hinsbergh VWM Van, Hyperpermeability E. Activation of RhoA by Thrombin in Endothelial Hyperpermeability. *Circulation Research*. 2000;87:335–340.
7. Xu M, Waters CL, Hu C, Wysolmerski RB, Vincent PA, Minnear FL. Sphingosine 1-phosphate rapidly increases endothelial barrier function independently of VE-cadherin but requires cell spreading and Rho kinase. *Am.J.Physiol Cell Physiol*. 2007;293(4):C1309–C1318.
8. Van Nieuw Amerongen GP, Beckers CML, Achekar ID, Zeeman S, Musters RJP, Van Hinsbergh VWM. Involvement of Rho kinase in endothelial barrier maintenance. *Arteriosclerosis, Thrombosis, and Vascular Biology*. 2007;27(11):2332–2339.
9. Gudermann T, Steinritz D. STIMulating stress fibers in endothelial cells. *Science signaling*. 2013;6(267):pe8.
10. Baumer Y, Burger S, Curry FE, Golenhofen N, Drenckhahn D, Waschke J. Differential role of Rho GTPases in endothelial barrier regulation dependent on endothelial cell origin. *Histochemistry and cell biology*. 2008;129(2):179–191.
11. Uhlig S, Yang Y, Waade J, Wittenberg C, Babendreyer A, Kuebler WM. Differential regulation of lung endothelial permeability in vitro and in situ. *Cellular Physiology and Biochemistry*. 2014;34(1):1–19.
12. Huveneers S, Oldenburg J, Spanjaard E, van der Krogt G, Grigoriev I, Akhmanova A, Rehmann H, de Rooij J. Vinculin associates with endothelial VE-cadherin junctions to control force-dependent remodeling. *The Journal of cell biology*. 2012;196(5):641–652.
13. Li X, Hahn CN, Parsons M, Drew J. Role of protein kinase Cζ in thrombin-induced endothelial permeability changes: inhibition by angiopoietin-1. *Hemostasis, Thrombosis, and Vascular Biology*. 2004;104(6):1716–1725.
14. van Nieuw Amerongen GP, Vermeer M a, van Hinsbergh VW. Role of RhoA and Rho kinase in lysophosphatidic acid-induced endothelial barrier dysfunction. *Arteriosclerosis, thrombosis, and vascular biology*. 2000;20(12):E127–E133.
15. Gorovoy M, Neamu R, Niu J, Vogel S, Predescu D, Miyoshi J, Takai Y, Kini V, Mehta D, Malik AB, Voyno-Yasenetskaya T. RhoGDI-1 modulation of the activity of monomeric RhoGTPase RhoA regulates endothelial barrier function in mouse lungs. *Circulation research*. 2007;101(1):50–58.
16. Satchi-Fainaro R, Mamluk R, Wang L, Short SM, Nagy JA, Feng D, Dvorak AM, Dvorak HF, Puder M, Mukhopadhyay D, Folkman J. Inhibition of vessel permeability by TNP-470 and its polymer conjugate, caplostatin. *Cancer Cell*. 2005;7(3):251–261.
17. Ding RY, Zhao DM, Zhang ZD, Guo RX, Ma XC. Pretreatment of Rho kinase inhibitor inhibits systemic inflammation and prevents endotoxin-induced acute lung injury in mice. *Journal of Surgical Research*. 2011;171(2):e209–e214.
18. McGown CC, Brown NJ, Hellewell PG, Brookes ZLS. ROCK induced inflammation of the microcirculation during endotoxemia mediated by nitric oxide synthase. *Microvascular Research*. 2011;81(3):281–288.
19. Riento K, Ridley AJ. Rocks: multifunctional kinases in cell behaviour. *Nature reviews. Molecular cell biology*. 2003;4(6):446–456.
20. Boerma M, Fu Q, Wang J, Loose DS, Bartolozzi A, Ellis JL, McGonigle S, Paradise E, Sweetnam P, Fink LM, Vozenin-Brotons M-C, Hauer-Jensen M. Comparative gene expression profiling in three primary human cell lines after treatment with a novel inhibitor of Rho kinase or atorvastatin. *Blood coagulation & fibrinolysis : an international journal in haemostasis and thrombosis*. 2008;19(7):709–718.
21. Thumkeo D, Keel J, Ishizaki T, Nonomura K, Oshima H, Taketo MM, Narumiya S, Hirose M. Targeted Disruption of the Mouse Rho-Associated Kinase 2 Gene Results in Intrauterine Growth Retardation and Fetal Death Targeted Disruption of the Mouse Rho-Associated Kinase 2 Gene Results in Intrauterine Growth Retardation and Fetal Death. *Molecular and cellular biology*. 2003;23(14):5043–5055.

22. Shimizu Y, Thumkeo D, Keel J, Ishizaki T, Oshima H, Oshima M, Noda Y, Matsumura F, Taketo MM, Narumiya S. ROCK-I regulates closure of the eyelids and ventral body wall by inducing assembly of actomyosin bundles. *Journal of Cell Biology*. 2005;168(6):941–953.
23. Loirand G, Guérin P, Pacaud P. Rho kinases in cardiovascular physiology and pathophysiology. *Circulation research*. 2006;98(3):322–334.
24. Zhou Q, Gensch C, Liao JK. Rho-associated coiled-coil-forming kinases (ROCKs): Potential targets for the treatment of atherosclerosis and vascular disease. *Trends in Pharmacological Sciences*. 2011;32(3):167–173.
25. Montalvo J, Spencer C, Hackathorn A, Masterjohn K, Perkins A, Doty C, Arumugam A, Ongusaha PP, Lakshmanaswamy R, Liao JK, Mitchell DC, Bryan BA. Rock1 & 2 Perform Overlapping and Unique Roles in Angiogenesis and Angiosarcoma Tumor Progression. *Curr Mol Med*. 2013;1:205–219.
26. Wang Y, Zheng XR, Riddick N, Bryden M, Zhang X, Surks HK. ROCK Isoform Regulation of Myosin Phosphatase and Contractility in Vascular Smooth Muscle Cells. *Circulation Research*. 2009;104(4):531–540.
27. McLaughlin JN, Shen L, Holinstat M, Brooks JD, DiBenedetto E, Hamm HE. Functional selectivity of G protein signaling by agonist peptides and thrombin for the protease-activated receptor-1. *Journal of Biological Chemistry*. 2005;280(26):25048–25059.
28. Breyer J, Samarin J, Rehm M, Lautscham L, Fabry B, Goppelt-Struebe M. Inhibition of Rho kinases increases directional motility of microvascular endothelial cells. *Biochemical Pharmacology*. 2012;83(5):616–626.
29. Chuang H-H, Yang C-H, Tsay Y-G, Hsu C-Y, Tseng L-M, Chang Z-F, Lee H-H. ROCKII Ser1366 phosphorylation reflects the activation status. *The Biochemical journal*. 2012;443(1):145–151.
30. van Nieuw Amerongen GP, Musters RJP, Eringa EC, Sipkema P, van Hinsbergh VWM. Thrombin-induced endothelial barrier disruption in intact microvessels: role of RhoA/Rho kinase-myosin phosphatase axis. *American journal of physiology. Cell physiology*. 2008;294(5):C1234–1241.
31. Trepat X, Deng L, An SS, Navajas D, Tschumperlin DJ, Gerthoffer WT, Butler JP, Fredberg JJ. Universal physical responses to stretch in the living cell. *Nature*. 2007;447(7144):592–595.
32. Krishnan R, Klumpers DD, Park CY, Rajendran K, Trepat X, van Bezu J, van Hinsbergh VWM, Carman C V, Brain JD, Fredberg JJ, Butler JP, van Nieuw Amerongen GP. Substrate stiffening promotes endothelial monolayer disruption through enhanced physical forces. *American journal of Cell physiology*. 2011;300(1):C146–C154.
33. Maruthamuthu V, Sabass B, Schwarz US, Gardel ML. Cell-ECM traction force modulates endogenous tension at cell – cell contacts. *Proc. Natl. Acad. Sci. USA*. 2011;108(12):4708–4713.
34. Goeckeler ZM, Bridgman PC, Wysolmerski RB. Nonmuscle myosin II is responsible for maintaining endothelial cell basal tone and stress fiber integrity. *Am J Physiol Cell Physiol*. 2008;26506:994–1006.
35. Tambe DT, Hardin CC, Angelini TE, Rajendran K, Park CY, Serra-Picamal X, Zhou EH, Zaman MH, Butler JP, Weitz D a, Fredberg JJ, Trepat X. Collective cell guidance by cooperative intercellular forces. *Nature materials*. 2011;10(6):469–475.
36. Bryan BA, Dennstedt E, Mitchell DC, Walshe TE, Noma K, Loureiro R, Saint-Geniez M, Campaigniac J-P, Liao JK, D'Amore P a. RhoA/ROCK signaling is essential for multiple aspects of VEGF-mediated angiogenesis. *FASEB journal : official publication of the Federation of American Societies for Experimental Biology*. 2010;24(9):3186–3195.
37. Moreno V, Gonzalo P, Gómez-Escudero J, Pollán Á, Acín-Pérez R, Breckenridge M, Yáñez-Mó M, Barreiro O, Orsenigo F, Kadomatsu K, Chen CS, Enríquez J a, Dejana E, Sánchez-Madrid F, Arroyo AG. An EMMPRIN-γ-catenin-Nm23 complex drives ATP production and actomyosin contractility at endothelial junctions. *Journal of cell science*. 2014;127:3768–3781.
38. Conway DE, Breckenridge MT, Hinde E, Gratton E, Chen CS, Schwartz M a. Fluid shear stress on endothelial cells modulates mechanical tension across VE-cadherin and PECAM-1. *Current biology*. 2013;23(11):1024–1030.
39. Borghi N, Sorokina M, Shcherbakova OG, Weis WI, Pruitt BL, Nelson WJ, Dunn AR. E-cadherin is under constitutive actomyosin-generated tension that is increased at cell-cell contacts upon externally applied stretch. *Proceedings of the National Academy of Sciences of the United States of America*. 2012;109(31):12568–12573.
40. Huveneers S, de Rooij J. Mechanosensitive systems at the cadherin-F-actin interface. *Journal of cell science*. 2013;126(2):403–413.
41. Daneshjou N, Sieracki N, van Nieuw Amerongen GP, Schwartz M a., Komarova Y a., Malik a. B. Rac1 functions as a reversible tension modulator to stabilize VE-cadherin trans-interaction. *The Journal of Cell Biology*. 2015;208(1):23–32.
42. Ivanov AI, Samarin SN, Bachar M, Parkos CA, Nusrat A. Protein kinase C activation disrupts epithelial apical junctions via ROCK-II dependent stimulation of actomyosin contractility. *BMC Cell Biology*. 2009;10(36).

43. Mong PY, Wang Q. Activation of Rho kinase isoforms in lung endothelial cells during inflammation. *Journal of immunology*. 2009;182(4):2385–2394.
44. Bogatcheva N V., Zemskova MA, Poirier C, Mirzapoiazova T, Kolosova I, Bresnick AR, Verin AD. The suppression of myosin light chain (MLC) phosphorylation during the response to lipopolysaccharide (LPS): Beneficial or detrimental to endothelial barrier? *Journal of Cellular Physiology*. 2011;226(12):3132–3146.
45. Klein AM, Dioum EM, Cobb MH. Exposing contingency plans for kinase networks. *Cell*. 2010;143(6):867–869.
46. Wageningen S Van, Kemmeren P, Lijnzaad P, Margaritis T, Benschop JJ, Castro IJ De, Leenen D Van, Koerkamp MJAG, Ko CW, Miles AJ, Brabers N, Brok MO, Lenstra TL, Fiedler D, Fokkens L, et al. Functional Overlap and Regulatory Links Shape Genetic Interactions between Signaling Pathways. *Cell*. 2010;143(6):991–1004.
47. Noma K, Rikitake Y, Oyama N, Yan G, Alcaide P, Liu P, Wang H, Ahl D, Sawada N, Okamoto R, Hiroi Y, Shimizu K, Luscinskas FW, Sun J, Liao JK. ROCK1 mediates leukocyte recruitment and neointima formation following vascular injury. *The Journal of Clinical Investigation*. 2008;118(5):1632–1644.
48. Burridge K, Wittchen ES. The tension mounts: Stress fibers as force-generating mechanotransducers. *The Journal of Cell Biology*. 2013;200(1):9–19.
49. van Geemen D, Smeets MWJ, van Stalborch A-MD, Woerdeman L a E, Daemen MJ a P, Hordijk PL, Huveneers S. F-Actin-Anchored Focal Adhesions Distinguish Endothelial Phenotypes of Human Arteries and Veins. *Arteriosclerosis, thrombosis, and vascular biology*. 2014;34(9):2059–2067.
50. Terry SJ, Zihni C, Elbediwy A, Vitiello E, Leefa Chong San I V, Balda MS, Matter K. Spatially restricted activation of RhoA signalling at epithelial junctions by p114RhoGEF drives junction formation and morphogenesis. *Nature cell biology*. 2011;13(2):159–166.
51. Farber MJ, Rizaldy R, Hildebrand JD. Shroom2 regulates contractility to control endothelial morphogenesis. *Molecular biology of the cell*. 2011;22(6):795–805.
52. Holinstat M, Knezevic N, Broman M, Samarel AM, Malik AB, Mehta D. Suppression of RhoA activity by focal adhesion kinase-induced activation of p190RhoGAP: Role in regulation of endothelial permeability. *Journal of Biological Chemistry*. 2006;281(4):2296–2305.
53. Tauseef M, Kini V, Knezevic N, Brannan M, Ramchandaran R, Fyrst H, Saba J, Vogel SM, Malik AB, Mehta D. Activation of sphingosine kinase-1 reverses the increase in lung vascular permeability through sphingosine-1-phosphate receptor signaling in endothelial cells. *Circulation research*. 2008;103(10):1164–1172.

Supplemental material

Detailed methods

Materials

EBM2 and medium Medium 199 supplemented with 20 mmol/L HEPES, L-glutamine and penicillin/streptomycin were obtained from Lonza (Basel, Switzerland); newborn calf serum (NBCS) was obtained from Gibco (Grand Island, NY). Tissue culture plastics were from Costar (Cambridge, MA). A crude preparation of endothelial cell growth factor (ECGF) was prepared from bovine hypothalamus as described by Maciag *et al.*.[1] Human serum albumin (HSA) and human serum were obtained from Sanquin CLB (Amsterdam, The Netherlands). Serum was prepared from 10 to 20 healthy donors, pooled, heat-inactivated and stored at 4°C. Trypsin was purchased from Gibco/Invitrogen (Grand island, NY), heparin from Leo Pharmaceutical Products (Weesp, The Netherlands) Thrombin from Sigma (Missouri, USA). Ac-TFLLRNPNDK-NH2 was from Biosource/Invitrogen (Carlsbad, CA). FITC- and HRP-labeled secondary antibodies were from Dako (Ostrup, Denmark). Rhodamine-phalloidin was from Molecular Probes (Eugene, Oregon). Antibodies against VE-cadherin, ROCK1 and ROCK2 were from Santa Cruz Biotechnology Inc. (Santa Cruz, CA). pS1366ROCK antibody was kind gift of dr.H.H. Lee (Taipei, Taiwan).[2] SLx-2119 was Surface Logix (Brighton, MA). Y-27632 was obtained from Calbiochem (Amsterdam, The Netherlands).

Cell Culture

Unless indicated otherwise, experiments were performed with human umbilical vein endothelial cells (HUVECs). Key findings were verified in human pulmonary microvascular endothelial cells (HPMVECs). HUVECs were isolated, cultured, and characterized as previously described.[3] HUVECs were cultured on fibronectin- or gelatin-coated dishes in Medium 199 supplemented with 20 mmol/L HEPES (pH 7.3), 10% heat-inactivated human serum, 10% heat-inactivated newborn calf serum, 40 µg/mL crude endothelial cell growth factor, 2 mmol/L L-glutamine, 5 U/mL heparin, 100 IU/mL penicillin, and 100 µg/mL streptomycin at 37°C under 5% CO^2 /95% air atmosphere. Media were changed every other day. Cells were cultured up to passage 2. Before all experiments cells were washed once with Medium 199 and preincubated for 1 hour in Medium 199 + 1% HSA.

Human pulmonary microvascular endothelial cells (HPMVECs) were isolated from human lung tissue, as previously described.[4] Cells were cultured in EGM2-MV culture medium (EBM2 medium supplemented with 5% fetal bovine serum, human epidermal growth factor, fibroblast growth factor, vascular endothelial growth factor, insulin-like growth factor, hydrocortisone, ascorbic acid, gentamicin and amphotericin according to the manufacturers protocol, and with 100 IU/mL penicillin and 100mg/mL streptomycin) and seeded on gelatine-coated 25cm^2 culture flasks. Cells were grown to confluence at 37^0C and 5% CO^2, with a change of culture medium every other day. They were extensively characterized as endothelial cells by the presence of endothelial markers and the absence of epithelial, lymphatic and smooth muscle cell markers. Cells were cultured up to passage 7, for experiments passage 4-7 cells were used.

HUVEC transfections

For *in vitro* studies of RNA interference, transfections were performed with *ROCK1*– and *ROCK2*–validated short interfering (si) RNA duplexes (50 nM) or a scrambled nonsilencing siRNA as negative control (Santa Cruz Biotechnology, Santa Cruz, CA). HUVECs were transfected using Amaxa nucleofection according to the manufacturer's protocol (www.amaxa.com) as described previously.[3] At 48 hours after siRNA transfection endothelial barrier function was evaluated or cells were harvested to determine the level of ROCK1 and ROCK2 proteins by immunoblotting. The efficiency of the transfection was monitored by immunoblotting 48 hours after transfection. A net decrease in ROCK protein expression in each experiment of at least 90% was observed in ROCK1-silenced ECs and of 75% in ROCK2-silenced ECs.

Western blotting

Proteins were separated by gel electrophoresis, blotted onto a nitrocellulose membrane, and stained with the indicated primary antibodies. Proteins were detected by chemi-luminescence according to the manufacturer's protocol (Amersham), and images were obtained using a charge-couple device camera (Fuji Science Imaging Systems). Signals were quantified with AIDA Image Analyzer software (Isotopenmessgeräte; Staubenhardt, Germany).

Evaluation of the barrier function

For the evaluation of the barrier function, confluent monolayers of HUVEC (first and second passage) were trypsinized and seeded in high density on polycarbonate filters of the Transwell™ system pre-coated with fibronectin and gelatin, and cultured. Medium was renewed every other day. Monolayers were used between 4 and 6 days after seeding. Passage of macromolecules across the endothelial monolayers during a one hour-period was investigated by assay of the transfer of HRP and was performed as described previously.[5] Preceding the HRP passage, monolayers were preincubated with the Rho kinase inhibitors (10 microM/L) Y-27632, and SLx-2119 for 30 minutes.

Electrical cell substrate impedance sensing (ECIS)

ECIS™ Model 1600R (Applied BioPhysics, Troy, NY, USA) was used to measure transendothelial electrical resistance (TEER) in confluent monolayers according to Tiruppathi *et al*..[6] In short, 250 µl of cell suspension ($8x10^5$ cells per ml) was seeded to each well of an 8W1 ECIS array equilibrated with cystein solution according to the manufacturer's protocol and coated with gelatin. When monolayers reached maximum resistance endothelial integrity was measured in real-time as described. Resistance was measured at multiple frequencies to allow for calculation of resistance attributable to cell-cell adhesion (Rb) and to cell-matrix interaction (Alpha).[7,8]

3D Digital imaging microscopy

EC were fixed with 2% formaldehyde in PBS for 10 minutes at room temperature, and stained for F-actin with rhodamine-phalloidin. Stained cells were washed in PBS and mounted in Vectashield® Mounting medium for fluorescence with DAPI from Vector Laboratories, Inc. (Burlingame, California, USA). Digital imaging microscopy was performed essentially as described before.[3] In short, HUVECs

were examined with a ZEISS Axiovert 200 Marianas inverted microscope, equipped with a motorized stage (stepper-motor z-axis increments: 0.1 micron). A cooled CCD camera [Cooke Sensicam (Cooke, Tonawanda, NY), 1280x1024 pixels] recorded images with true 16-bit capability. The camera is linear over its full dynamic range (up to intensities of over 4000) while dark/background currents (estimated by the intensity outside the cells) are typically < 100. Exposures, objective, montage, and pixel binning were automatically recorded with each image stored in memory. The microscope, camera, data viewing/processing were conducted/controled by SlidebookTM software (Intelligent Imaging Innovations, Denver, CO). Images were taken with a custom ZEISS 40x air (NA 0.75) and 63X oil lens (NA 1.4).

Quantification of monolayer contractility

To measure EC monolayer contraction, we used monolayer traction microscopy.[9] Briefly, ECs were seeded cells at confluence on 4kPa stiff collagen-coated polyacrylamide gel substrates. Within those gels, we embedded fluorescent microbeads. Images of microbeads obtained during the experiment were compared with a second image of the same microbeads obtained after detachment of cells at the end of the experiment. From these two images, a monolayer displacement field was computed. From the displacement field, we computed the monolayer traction field.[10] This computation circumvents limitations of the classical boundary value problem [11] through a new algorithm that accounts for unbalanced forces within the microscope field of view. From the traction field, we calculated the root mean square (RMS) value of monolayer traction. RMS tractions were reported for the following groups: Control, SLx-2119 pretreatment, and Y-27632 pretreatment. The monolayers were subsequently treated with thrombin and RMS tractions were computed 10 minutes after treatment.

Quantification of intercellular stress

To measure intercellular stress in intact monolayers we used Monolayer Stress Microscopy as previously described.[12] Briefly, each cell in the monolayer exerts local forces on the substrate (here called traction forces) which are balanced across the entire monolayer – giving rise to the local intercellular stress. Since the lateral extent of the monolayers studied here is much greater than their height we calculate the force balance in two demensions by treating the monolayer as a continuous, 2-D ,thin elastic sheet. The local intercellular stress at any point in the sheet is represented by the local stress tensor, σ_{ij} where i,j run over the coordinates x,y. Stresses in the Z direction are assumed to be zero. As above, there is no net force on the monolayer, σ_{ij} balances the measured traction forces and the key equation giving the intercellular force becomes:

$$\frac{\partial \sigma_{ij}}{\partial x_j} = T_i$$

Where we sum over repeated indices. The only assumption in the above treatment is that the monolayer can be treated as a continuum. However, since in the present work we study cells in the interior of the monolayer a problem arises at the boundary of the field of view where we do not know the stresses. We impose a boundary condition of zero normal displacement, which could lead

to inaccurate calculation of intercellular forces close to the edge. We have previously shown that the intercellular forces are dominated by the local source terms (the tractions) and any influence from cells outside of the field of view generally decays as 1/r where r is the distance from the edge.[12] In the stress maps presented, we have discarded the calculated stresses from a region roughly 100 µm wide around the outer edge of the image, thus minimizing this error.

Liposomal delivery of siRNA in the mouse lung

Cationic liposomes were made using a mixture of dimethyldioctadecyl-ammonium bromide (DDAB) and cholesterol in chloroform, as described previously.[13] Control, ROCK1 or ROCK2 siRNA (75 µg) or ROCK1 + ROCK2 (37.5 µg each siRNA) were mixed with 100 µL of liposomes. As the ROCK1 and ROCK2 that were used for *in vitro* studies with human ECs were less effective in cultured mouse NIH3T3 cells, we designed new siRNAs (siRNAROCK1: CUACCACUUUCCUGCCAAUUU and siRNA ROCK2: UGAAGAAAGUCAAGAGAU (Dharmacon, Herlev, Denmark)), that resulted in a >80% downregulation of ROCK1 and ROCK2 *in vitro*, Figure 1. The mixture of liposomes and siRNA were injected intravenously (via retro-orbital injection) into C57/Bl6 mice. After 48 hrs mice were used for determining lung microvascular permeability or were used for immunoblotting and immunohistochemistry analysis.

Assessment of lung capillary leakage

PAR1 specific peptide (TFRLLN) (1 mg/kg) or control peptide (FTLLRN) was injected retroorbitally followed by injection of Evans blue conjugated albumin (EBA) (20 mg/kg) as described.[14,15] After 30 min, mice were sacrificed and blood was collected from the right ventricle into heparinized syringes. Plasma was separated by centrifugation at 1,300 x *g* for 10 minutes. Right lung lobe was homogenized as described.[15] Lung homogenates and plasma were incubated with 2 volumes of formamide (18 hr, 60°C), centrifuged at 5,000 x *g* for 30 min, and the optical density of the supernatant was determined spectrophotometrically at 620 nm and at 740 nm (to correct for hemoglobin). EBA extravasation was calculated as the ratio of EBA extravasated in lung versus that in plasma.

Lung weight determination

Left lungs from the same mice used for EBA extravasation were excised and completely dried in the oven at 60°C overnight for calculation of lung wet-dry ratio.[16]

Immunohistochemistry

Right lungs were flushed with saline and embedded in paraffin. For immunohistochemistry 5µm slices were cut and stained for ROCK1 and ROCK2. In short, paraffin slices were deparaffinized with xylene, and rehydrated with 100% ethanol. Endogenous peroxydase was blocked with 0.3% H_2O_2/methanol solution. After antigen retrieval (60min autoclave in 10mM sodium-citrate solution, pH 6.0), slices were overnight (4°C) incubated with primary antibody against ROCK1 (1:100, #611136, BD Transduction Laboratories, New Jersey, USA), ROCK2 (1:250, #610623, BD Transduction Laboratories), or antibody diluent alone (negative control). Detection of primary antibody was performed with Envision® (ROCK1, DAKO Netherlands, Heverlee, Belgium) or Powervision® (ROCK2, Immunologic, Duiven, The Netherlands), according to the manufacturers protocol, and subsequently counterstained

with hematoxylin. Slices were evaluated with a Leica DMRB light microscope (Leica Microsystems, Wetzlar, Germany) at 20x (air, NA 0.40) and 40x (air, NA 0.65) magnification. For imaging, a Nikon D50 digital camera (Nikon Corporation, Tokyo, Japan) was used. For quantification, line scans were drawn over the vessel wall from the lumen to the cytosplasm of underlying smooth muscle cells (see Figure 1C). Staining intensity over the line scan was calculated using Image J software. The intensity of staining in the endothelial cell layer was compared with luminal staining intensity (background signal) and with cytoplasmic staining intensity of smooth muscle cells (as non-targeted tissue). The difference in staining intensity with smooth muscle cells was used to measure effectivity of knock down of indicated siRNAs. Effectivity of knockdown was measured in arterioles. Per arteriole three line scans were drawn, and the average staining intensity (endothelial cell – smooth muscle cell) was taken.

Statistical analysis

All data are reported as mean ± SD. Comparisons between 2 experimental groups were made by student t-test and between >2 groups by one way ANOVA with bonferoni post-hoc test. Differences in mean values were considered significant at $p < 0.05$.

Reference List

1. Maciag T, Cerundolo J, Ilsley S, Kelley PR, Forand R. An endothelial cell growth factor from bovine hypothalamus: identification and partial characterization. *Proceedings of the National Academy of Sciences of the United States of America*. 1979;76(11):5674–5678.
2. Chuang H-H, Yang C-H, Tsay Y-G, Hsu C-Y, Tseng L-M, Chang Z-F, Lee H-H. ROCKII Ser1366 phosphorylation reflects the activation status. *The Biochemical journal*. 2012;443(1):145–151.
3. Van Nieuw Amerongen GP, Beckers CML, Achekar ID, Zeeman S, Musters RJP, Van Hinsbergh VWM. Involvement of Rho kinase in endothelial barrier maintenance. *Arteriosclerosis, Thrombosis, and Vascular Biology*. 2007;27(11):2332–2339.
4. Shelton JL, Wang L, Cepinskas G, Sandig M, Inculet R, McCormack DG, Mehta S. Albumin leak across human pulmonary microvascular vs. umbilical vein endothelial cells under septic conditions. *Microvascular Research*. 2006;71(1):40–47.
5. Van Nieuw Amerongen G, Van Hinsbergh V. Determination of the endothelial barrier function in vitro. *Methods Mol Biol.* 1999;96:183–189.
6. Tiruppathi C, Malik a B, Del Vecchio PJ, Keese CR, Giaever I. Electrical method for detection of endothelial cell shape change in real time: assessment of endothelial barrier function. *Proceedings of the National Academy of Sciences of the United States of America*. 1992;89(17):7919–7923.
7. Moy AB, Winter M, Kamath A, Blackwell K, Reyes G, Giaever I, Keese C, Shasby DM. Histamine alters endothelial barrier function at cell-cell and cell-matrix sites. *American journal of physiology. Lung cellular and molecular physiology*. 2000;278(5):L888–L898.
8. Aman J, van Bezu J, Damanafshan A, Huveneers S, Eringa EC, Vogel SM, Groeneveld a BJ, Vonk Noordegraaf A, van Hinsbergh VWM, van Nieuw Amerongen GP. Effective treatment of edema and endothelial barrier dysfunction with imatinib. *Circulation*. 2012;126(23):2728–2738.
9. Trepat X, Wasserman MR, Angelini TE, Millet E, Weitz DA, Butler JP, Fredberg JJ. Physical forces during collective cell migration. *Nature Physics*. 2009;5(6):426–430.
10. Trepat X, Deng L, An SS, Navajas D, Tschumperlin DJ, Gerthoffer WT, Butler JP, Fredberg JJ. Universal physical responses to stretch in the living cell. *Nature*. 2007;447(7144):592–595.
11. Krishnan R, Klumpers DD, Park CY, Rajendran K, Trepat X, van Bezu J, van Hinsbergh VWM, Carman C V, Brain JD, Fredberg JJ, Butler JP, van Nieuw Amerongen GP. Substrate stiffening promotes endothelial monolayer disruption through enhanced physical forces. *American journal of Cell physiology*. 2011;300(1):C146–C154.
12. Tambe DT, Hardin CC, Angelini TE, Rajendran K, Park CY, Serra-Picamal X, Zhou EH, Zaman MH, Butler JP, Weitz D a, Fredberg JJ, Trepat X. Collective cell guidance by cooperative intercellular forces. *Nature materials*. 2011;10(6):469–475.
13. Holinstat M, Knezevic N, Broman M, Samarel AM, Malik AB, Mehta D. Suppression of RhoA activity by focal adhesion kinase-induced activation of p190RhoGAP: Role in regulation of endothelial permeability. *Journal of Biological Chemistry*. 2006;281(4):2296–2305.
14. Peng X, Hassoun PM, Sammani S, McVerry BJ, Burne MJ, Rabb H, Pearse D, Tuder RM, Garcia JGN. Protective effects of sphingosine 1-phosphate in murine endotoxin-induced inflammatory lung injury. *American journal of respiratory and critical care medicine*. 2004;169(11):1245–1251.
15. Tauseef M, Kini V, Knezevic N, Brannan M, Ramchandaran R, Fyrst H, Saba J, Vogel SM, Malik AB, Mehta D. Activation of sphingosine kinase-1 reverses the increase in lung vascular permeability through sphingosine-1-phosphate receptor signaling in endothelial cells. *Circulation research*. 2008;103(10):1164–1172.
16. Barnard JW, Biro MG, Lo SK, Ohno S, Carozza MA, Moyle M, Soule HR, Malik AB. Neutrophil inhibitory factor prevents neutrophil-dependent lung injury. *Journal of immunology (Baltimore, Md. : 1950)*. 1995;155(10):4876–4881.

Supplemental figures

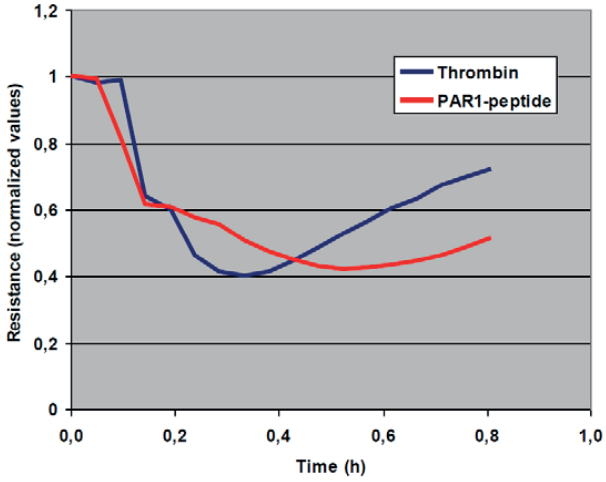

Figure S1. The endothelial barrier-disruptive effects of thrombin are recapitulated by activation of the thrombin receptor PAR1 with a PAR1-activating peptide. Representative tracings of alterations in trans-endothelial electrical resistance of HUVEC monolayers evoked by 1 U/mL thrombin (blue) and 45 µg/mLPAR1-peptide (red), as measured by the ECIS method, see Materials and Methods section.

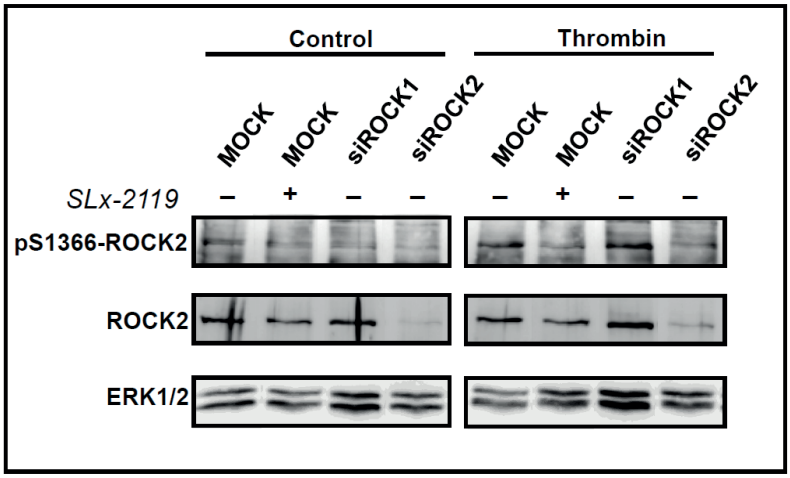

Figure S2. Thrombin-induced ROCK2 activation in HUVECs is ablated by the ROCK2 inhibitor SLx-2119, and by siROCK2, but not siROCK1. Representative Western blot showing changes in the phosphorylation of ROCK2 upon stimulation with 1U/mL thrombin for the indicated time points in the presence or absence of 10 microM SLx-2119 as indicated. Blot was probed with a phospho-specific ROCK2 antibody (upper panel). Blot was reprobed with ROCK2 (middle panel) antibody to verify reduced ROCK2 expression upon siRNA transfection and with ERK1/2 antibody (lower panel) as a loading control.

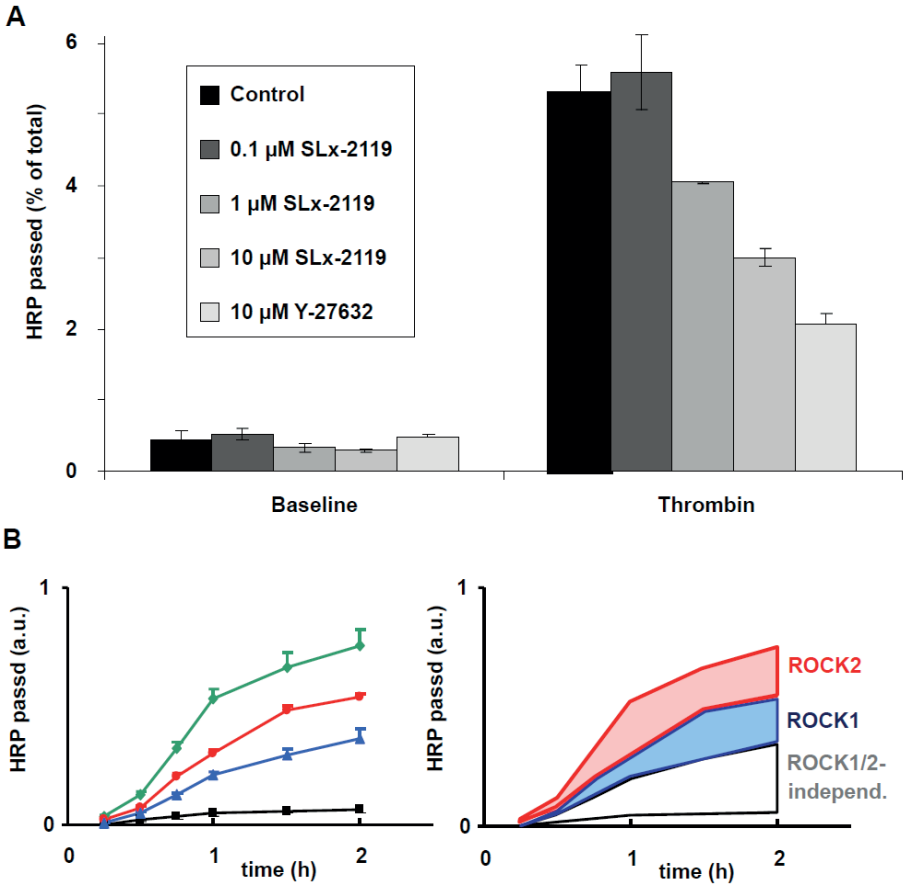

Figure S3 Dose- and time dependency of the effects of SLx-2119 on hyperpermeability of primary human pulmonary microvascular endothelial cell (HPMVEC) monolayers. (A) Representative experiment showing the effect of 0.1, 1 and 10 microM SLx-2119 and 10 microM Y-27632 on (thrombin-enhanced) HRP passage across HPMVEC monolayers. (B) Time-dependent effects of Rho kinase inhibitors on the passage of HRP across control and thrombin-stimulated human pulmonary microvascular endothelial monolayers. Confluent monolayers were preincubated for 1 hour in medium 199+1% HSA, pre-treated with 10 microM Y-27632 (blue), 10 microM SLx-2119 (red) or sham-treated (blue) for 30 minutes. Subsequently, the cumulative HRP passage across the monolayers was measured in the presence of 1 U/mL thrombin, as described in Materials and Methods. The baseline permeability of monolayers that were not treated with thrombin is shown for comparison (black). Right panel is color-shaded to better visualize the individual contributions of ROCK1 and ROCK2 to the thrombin-enhanced permeability. Values are the mean + SD (experiment performed in triplicate).

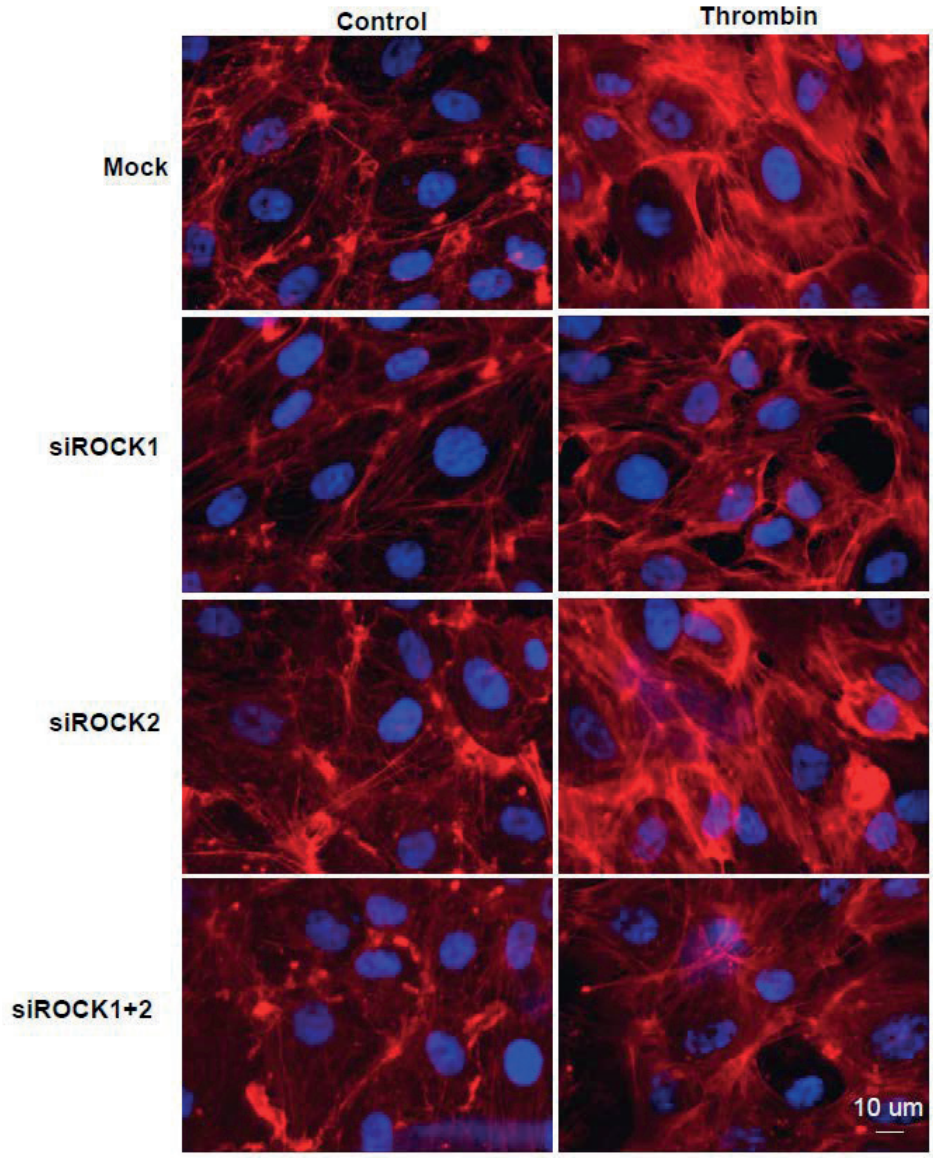

Figure S4. Effect of silencing of ROCK1 and/or ROCK2 on thrombin-induced changes in the F-actin cytoskeleton. HUVECS were treated with siRNAs for ROCK1 and ROCK2 as described in the Materials & Methods section, seeded on glass cover slips in a confluent density and grown for 48 hrs. ECs were preincubated for 1 hour in medium 199 + 1% HSA, subsequently stimulated for 30 minutes with 1 U/mL thrombin or sham-treated, and subsequently fixed with paraformaldehyde. HUVECs were stained for F-actin by rhodamine-phalloidin (red). Nuclei were stained with DAPI (blue).

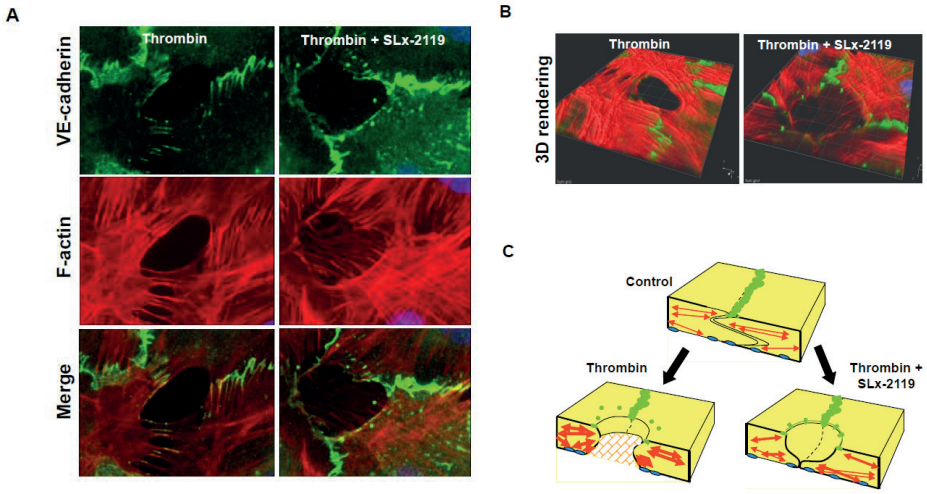

Figure S5. (A) Protrusive activity of ROCK2-inhibited HUVECs in thrombin-induced inter-endothelial gaps. Shown are enlarged images from the boxed areas in Figure 3. (B) 3D images were constructed by the 3D rendering mode in Slidebook software and show thin protrusion close to the glass surface. (C) Cartoon showing the protrusion filling inter-endothelial gaps in ROCK2-inhibited endothelial cells.

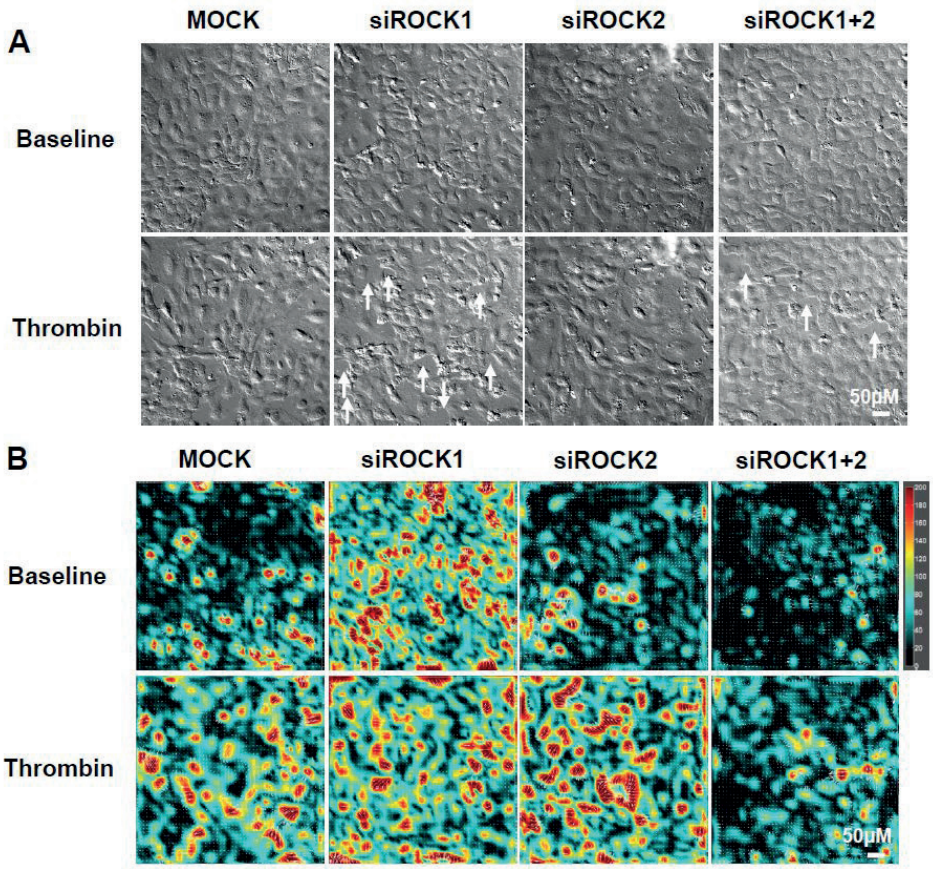

Figure S6. Silencing of ROCK2 does not affect thrombin-induced contractile stress enhancements. Representative phase contrast images (A) and cell-substrate traction stress maps (B), at baseline and post thrombin treatment from each group. Traction force microscopy was preformed 72 hours post-transfection for 15 minutes (baseline) and subsequently stimulated with thrombin (1 U/mL) for 30 min. Inter-endothelial gap are indicated with arrows. Bar = 50 um.